Electronic structure of $FeCr_2S_4$ and $Fe_{0.5}Cu_{0.5}Cr_2S_4$

2000 J. Phys.: Condens. Matter 12 5411

(http://iopscience.iop.org/0953-8984/12/25/306)

J. Phys.: Condens. Matter **12** (2000) 5411–5421. Printed in the UK PII: S0953-8984(00)12819-X

Electronic structure of $FeCr_2S_4$ and $Fe_{0.5}Cu_{0.5}Cr_2S_4$

E Z Kurmaev†, A V Postnikov†‡, H M Palmer§¶, C Greaves§,
St Bartkowski‡, V Tsurkan‖, M Demeter‡, D Hartmann‡, M Neumann‡,
D A Zatsepin†, V R Galakhov†, S N Shamin† and V Trofimova†

† Institute of Metal Physics, Russian Academy of Sciences—Ural Division,
620219 Yekaterinburgh GSP-170, Russia
‡ Universität Osnabrück, Fachbereich Physik, D-49069 Osnabrück, Germany
§ School of Chemistry, University of Birmingham, Birmingham, UK
‖ Institute of Applied Physics, Academy of Sciences of Moldova, Kishinev MD 2028,
Republic of Moldova

E-mail: h.m.palmer@bham.ac.uk

Received 24 March 2000

Abstract. A full study of the electronic structures of $FeCr_2S_4$ and $Fe_{0.5}Cu_{0.5}Cr_2S_4$ is reported based on x-ray photoelectron spectra (valence band and core levels), x-ray emission spectra (Fe Lα, Cu Lα, Cr Lα, S K$\beta_{1,3}$ and S $L_{2,3}$) and *ab initio* TB-LMTO band structure calculations. In the valence band of $FeCr_2S_4$, the Fe 3d states are found to be more localized than the Cr 3d states, which dominate at the Fermi level. In $Fe_{0.5}Cu_{0.5}Cr_2S_4$, the distribution of Cr 3d (Cr^{3+}) states is unchanged and the Cu ions were found to be in the Cu^+ state.

1. Introduction

The discovery of colossal magnetoresistance (CMR) in $Fe_{0.5}Cu_{0.5}Cr_2S_4$ and $FeCr_2S_4$ [1] has rekindled significant interest in Cr-based thiospinels, in particular their fundamental structural, electronic and magnetic properties [2] and band description. $FeCr_2S_4$ and $CuCr_2S_4$ form a series of solid solutions, whose basic electrical and magnetic properties were studied 30 years ago [3, 4]. The tetrahedral (Fe,Cu) and octahedral (Cr) sites in these thiospinels have opposed magnetic moments below T_c, giving rise to ferrimagnetic materials except for $CuCr_2S_4$, which is ferromagnetic. With respect to electrical properties, $FeCr_2S_4$ and $Fe_{0.5}Cu_{0.5}Cr_2S_4$ show p- and n-type semiconducting behaviour, respectively, while $CuCr_2S_4$ is metallic [4]. Given the CMR characteristics of both $FeCr_2S_4$ and $Fe_{0.5}Cu_{0.5}Cr_2S_4$, the influence of the charge carriers (their nature and concentration) on electrical and magnetic properties is of primary interest.

The nominal ionic composition of $FeCr_2S_4$ is well established as $Fe^{2+}Cr_2^{3+}S_4^{2-}$. For $CuCr_2S_4$ two different models have been proposed by Lotgering *et al* [4, 5] and Goodenough [6]. The first model claimed that the Cu should be monovalent, whereas the second claimed that Cu should be divalent. The substitution of Cu for Fe leads to a more complex situation with several possible electronic models, which depend on whether Cu enters as Cu^+ or Cu^{2+} ions. Unfortunately, this question remains so far unresolved. Whereas the introduction of Cu^{2+} would have no major impact on the charge distribution, various charge balance mechanisms are possible following the replacement of Fe^{2+} by Cu^+. For example, additional holes may

¶ Correspondence to Dr H M Palmer, School of Chemistry, University of Birmingham, Birmingham B15 2TT, UK.

0953-8984/00/255411+11$30.00

reside on Fe (giving Fe^{3+}), Cr (giving Cr^{4+}) or S (giving S^{-}). These possibilities have been the focus of several previous discussions [3, 4] as has been recently discussed by Min Sik Park *et al* [7], who reported band structure calculations for this system. In order to check the validity of the possible models, a full study of the x-ray photoelectron (XPS) and x-ray emission (XES) spectra of $FeCr_2S_4$ and $Fe_{0.5}Cu_{0.5}Cr_2S_4$ has been performed, and the implications compared with the results from *ab initio* TB-LMTO band structure calculations. In contrast to the data presented by Min Sik Park *et al* [7], which were based on an averaged structural model, the present calculations for $Fe_{0.5}Cu_{0.5}Cr_2S_4$ were performed on the correct structure with fully ordered Fe and Cu on the tetrahedral sites.

2. Experimental and calculation details

Single crystals of $FeCr_2S_4$ and $Fe_{0.5}Cu_{0.5}Cr_2S_4$ and polycrystalline $Fe_{0.5}Cu_{0.5}Cr_2S_4$ samples were used. Single phase $FeCr_2S_4$ and $Fe_{0.5}Cu_{0.5}Cr_2S_4$ polycrystals obtained from a solid state reaction of the elements were placed in a quartz ampoule (20 mm i.d. and 15 cm long) together with the transport agent (150–250 mg $CrCl_3$). Once evacuated, the ampoule was heated in a two zone furnace at 800–850 °C for pure and 900–950 °C for Cu substituted crystals. After 15–25 days octahedral (maximum size = 4 mm) and platelike (maximum size = 6 mm) single crystals were formed.

Magnetic properties of the samples were studied using a PAR 4500 vibrating sample magnetometer and magnetic fields of up to 1.6 T.

S $L_{2,3}$ x-ray emission spectra (valence $3s, 3d \rightarrow 2p$ transition) of $FeCr_2S_4$ and $Fe_{0.5}Cu_{0.5}Cr_2S_4$ were measured with an ultrasoft x-ray spectrometer [8] with high spatial (ΔS = 4–5 μm) and energy (ΔE = 0.4 eV) resolution using electron excitation. For the analysis of the x-radiation, a diffraction grating was used (N = 600 lines mm^{-1}; R = 2 m). The accelerating voltage on the x-ray tube was 4 keV and the anode current was 0.13 mA.

The Fe Lα, Cr Lα, and Cu Lα x-ray emission spectra (valence $3d, 4s \rightarrow 2p_{3/2}$ transition) were obtained by electron excitation and measured on a RSM-500-type x-ray vacuum spectrometer with a diffraction grating (N = 600 lines mm^{-1}; R = 6 m). The spectra were recorded in the second order of reflection by a secondary electron multiplier with a CsI photocathode. The instrumental resolution was ~0.35–0.40 eV for Fe Lα, Cr Lα and Cu Lα spectra. The x-ray tube was operated at 4 keV and 0.4 mA.

The S Kβ_1 x-ray emission spectrum (valence $3p \rightarrow 1s$ transition) was measured using a fluorescent Johan-type vacuum spectrometer with position-sensitive detector [9]. The Pd L x-radiation from a sealed x-ray tube was used for the excitation of the fluorescent S Kβ_1 spectra. A quartz (1010) single crystal, curved to R = 1400 mm, was used to disperse the radiation. X-rays were generated at 25 keV/50 mA and the spectra measured with an energy resolution of ~0.25 eV.

XPS measurements on $FeCr_2S_4$ and $Fe_{0.5}Cu_{0.5}Cr_2S_4$ were performed using a Physical Electronics PHI 5600 ci spectrometer (monochromatized Al Kα radiation with a 0.3 eV FWHM). The energy resolution of the analyser was 1.5% of the pass energy. The energy resolution was estimated to be better than 0.35 eV for the XPS measurements and the pressure in the vacuum chamber during the measurements was below 5×10^{-9} mbar. The samples were cleaved *in situ* under ultra-high vacuum prior to the XPS measurements. All the investigations were performed at room temperature on the freshly cleaved surfaces. The XPS spectra were calibrated using gold foil to obtain photoelectrons from the Au $4f_{7/2}$ subshell (binding energy 84.0 eV).

Band structure calculations were performed using the first-principles tight-binding linear muffin-tin orbitals method (TB-LMTO) [10–12]. The space group of $FeCr_2S_4$ is $Fd3m$ with

eight formula units per unit cell. Structural details for the calculations were obtained from Rietveld refinement based on x-ray powder diffraction data: $a = 9.9944(4)$ Å, Fe in 8a sites, Cr in 16d sites and S in 32e positions with $x = 0.2584(3)$. A full description of the structure will be presented elsewhere [13].

The calculations were based on the primitive cell containing two formula units, with additional empty spheres being introduced in the 16c and 48f (with $x = 0.891$) positions of the space group, resulting in a total of 30 sites for the calculations. In $Fe_{0.5}Cu_{0.5}Cr_2S_4$, the tetrahedral cations (Fe and Cu) have been found to be ordered [2], giving a symmetry reduction to the space group $F\bar{4}3m$. The structural data used have been previously reported [2]: $a = 9.9071(1)$ Å, Fe in 4a sites, Cu in 4d, Cr in 16e with $x = 0.3749(3)$. The ordering splits the sulphur positions into two inequivalent groups, S1 (16e) with $x = 0.1317(1)$ and S2 (16e) with $x = 0.6148(1)$. Additional empty spheres were again introduced at 16e ($x = 0.875$), 24f ($x = 0.248$) and 24g ($x = 0.999$) to provide 30 sites in all. The radii adopted for the space-filling atomic spheres were 2.502 (Fe), 2.656 (Cr) and 2.390 (S) au for $FeCr_2S_4$, and 2.473 (Fe, Cu), 2.553 (Cr), 2.378 (S1) and 2.439 (S2) for $Fe_{0.5}Cu_{0.5}Cr_2S_4$. Slightly smaller radii were used for the empty spheres. The local-density approximation for the exchange correlation after von Barth and Hedin [14] was used in the calculations, and non-local corrections after Langreth and Mehl [15, 16] were included. The density of states was calculated by the tetrahedron method with the $12 \times 12 \times 12$ divisions of the full Brillouin zone.

3. Results and discussion

3.1. Structural and magnetic properties

X-ray diffraction revealed the single phase spinel structure of the samples. The ferrimagnetic transition temperatures for the samples were determined from magnetization data (figures 1(a) and (b)) measured in low fields and found to be 348(1) K in $Fe_{0.5}Cu_{0.5}Cr_2S_4$ and 168(0.5) K in $FeCr_2S_4$. Both transition temperatures are in satisfactory agreement with previously published values of 340 K [1] and 349(5) K [17] for $Fe_{0.5}Cu_{0.5}Cr_2S_4$ and 180 K [1] for $FeCr_2S_4$.

Magnetic moments for the magnetically ordered structures of $Fe_{0.5}Cu_{0.5}Cr_2S_4$ and $FeCr_2S_4$ at 10 K, as have been obtained from neutron diffraction data [13] are $\mu(\mathrm{Fe}) = 3.1(1)\ \mu_B$, $\mu(\mathrm{Cr}) = 2.87(6)\ \mu_B$ and $\mu(\mathrm{Fe}) = 3.89(8)\ \mu_B$, $\mu(\mathrm{Cr}) = 2.71(5)\ \mu_B$, respectively.

3.2. XPS and XES spectra

Cu 2p and S 2p XPS spectra are shown in figure 2. Since the Cu 2p binding energy of $Fe_{0.5}Cu_{0.5}Cr_2S_4$ is closer to that in Cu_9O_5 (nonstoichiometric Cu_2O) and $CuFeO_2$ than to that of CuO[18], it can be concluded that the oxidation state of Cu in $Fe_{0.5}Cu_{0.5}Cr_2S_4$ is close to Cu^+. A characteristic feature of XPS 2p spectra of Cu^{2+} compounds is the presence of a high energy satellite structure that is found, for example in CuO and high-T_c superconducting cuprates [18, 19]. As seen from figure 2, this structure is absent in the XPS Cu 2p spectra of $Fe_{0.5}Cu_{0.5}Cr_2S_4$. Moreover, no exchange splitting was observed for the Cu 3s state, indicating a $3d^{10}$ configuration of the Cu^+ ion [20].

The Fe oxidation state in $FeCr_2S_4$ was determined from XPS measurements on a good quality single crystal and was found to be close to Fe^{2+} (figure 3). The introduction of Cu^+ into the structure should lead to the appearance of the Fe^{3+} signals in the Fe 2p XPS spectrum. For $Fe_{0.5}Cu_{0.5}Cr_2S_4$, both polycrystals and single crystals, the Fe 2p spectra are identical and they are very similar to the $FeCr_2S_4$ (Fe^{2+}) spectrum. This could be explained by a charge transfer from the S^{2-} to the Fe^{3+} ions during the photoemission excitation process

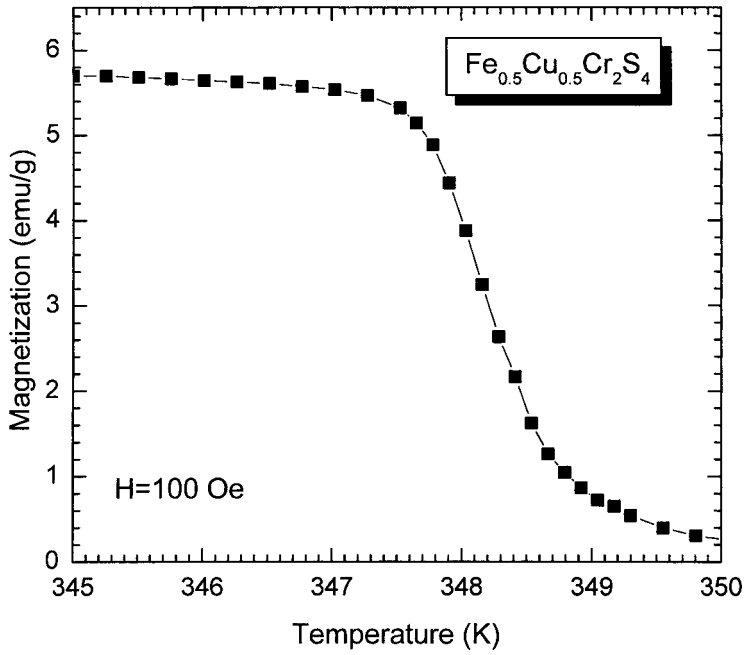

(a)

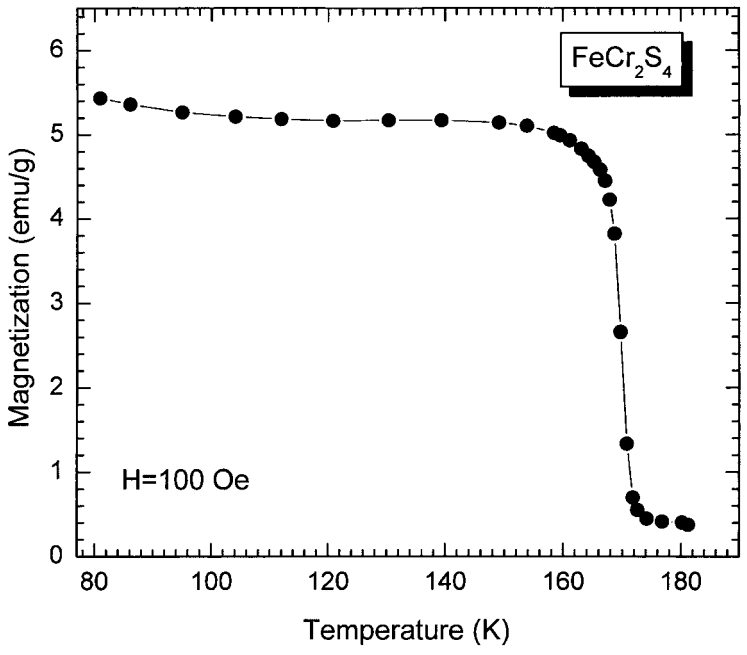

(b)

Figure 1. Magnetization versus temperature for the single crystals $Fe_{0.5}Cu_{0.5}Cr_2S_4$ (a) and $FeCr_2S_4$ (b).

such that photoemission would then imply a $Fe^{2+}S^{-}$ state. In the ground state no significant charge transfer is found. Magnetic measurements showed the existence of the Fe^{3+} ions [2].

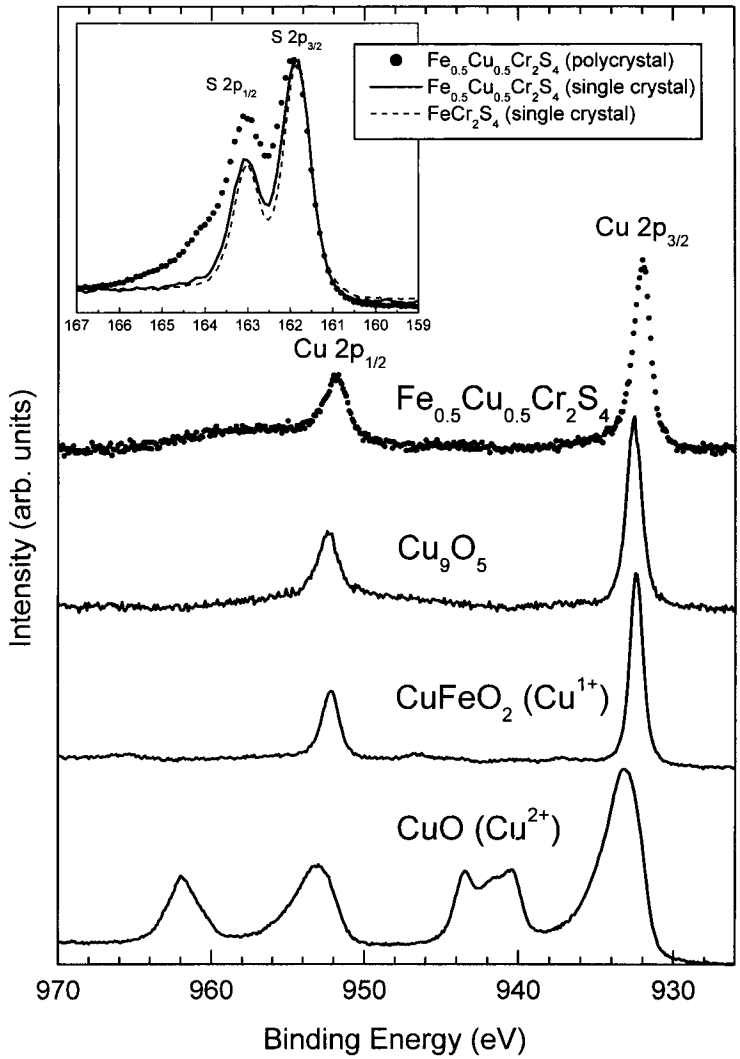

Figure 2. Main panel: Cu 2p XPS spectra in $Fe_{0.5}Cu_{0.5}Cr_2S_4$ and other Cu-containing compounds; inset: S 2p XPS spectra in $Fe_{0.5}Cu_{0.5}Cr_2S_4$ and $FeCr_2S_4$.

The S $2p_{3/2,1/2}$ XPS spectra of polycrystalline $Fe_{0.5}Cu_{0.5}Cr_2S_4$ (figure 2) show some differences with respect to the spectrum of $FeCr_2S_4$, which could be attributed to the appearance of an additional weak S $2p_{3/2,1/2}$ doublet, with an energetic position very close to that of FeS_2 (S^-). However, these states are most likely induced by defects. The spectra of crystalline material show no additional S^- features because of the delocalized nature of the S states.

These findings therefore imply that the introduction of Cu into $FeCr_2S_4$ mainly affects the Fe and S ions, but does not cause significant changes to the distribution of the Cr 3d (Cr^{3+}) states.

XPS valence bands (VBs) of $FeCr_2S_4$ and $Fe_{0.5}Cu_{0.5}Cr_2S_4$ measured in the range 0–16 eV are shown in figure 4. These spectra are normalized to the integrated intensity of the S 3s band, which is usually located at 11–16 eV in transition metal sulphides [21, 22]. According to

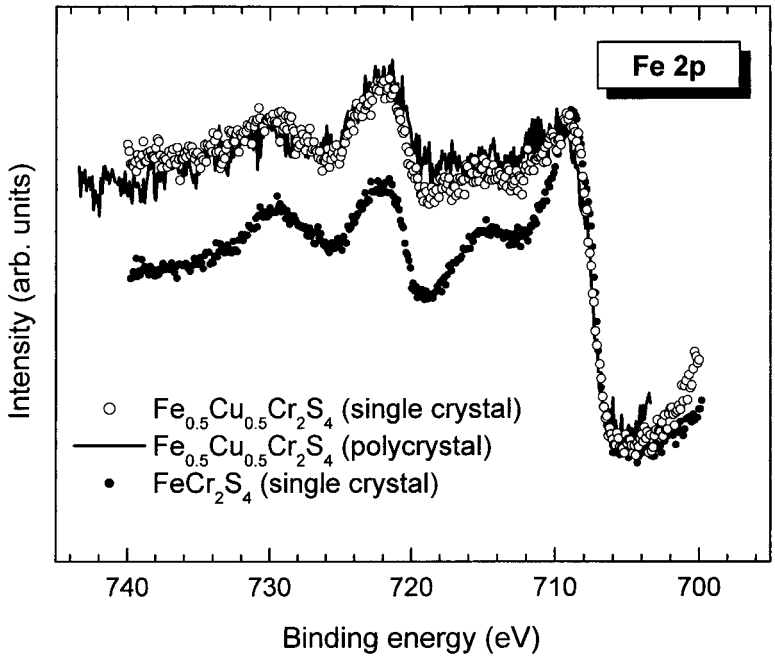

Figure 3. Fe 2p XPS spectra in $Fe_{0.5}Cu_{0.5}Cr_2S_4$ and $FeCr_2S_4$.

our analysis of the electronic structure of CuS, FeS_2, $CuFeS_2$ [22] and CuV_2S_4 [21], the energy difference between the S 3s and S 3p bands is ∼9 eV. The spectral feature of the XPS VBs of $FeCr_2S_4$ and $Fe_{0.5}Cu_{0.5}Cr_2S_4$ at ∼4 eV can therefore be attributed to the S 3p band. Since the Cr 3d states are expected to be less localized than the Fe 3d states in $FeCr_2S_4$ and $Fe_{0.5}Cu_{0.5}Cr_2S_4$, the features at about 1–1.5 and ∼6 eV can be assigned to the Cr 3d and Fe 3d states, respectively. The difference between the XPS VBs of $FeCr_2S_4$ and $Fe_{0.5}Cu_{0.5}Cr_2S_4$ is consistent with the presence of Cu 3d states located at ∼2 eV. The magnitude of the contribution from these states can be related to the large photoionization cross sections of Cu 3d states with respect to those of Cr 3d, Fe 3d, S 3p and S 3s states [23].

Fe Lα, Cr Lα, Cu Lα XES spectra (valence 3d4s $\rightarrow$ $2p_{3/2}$ transition) were recorded in order to estimate directly the contributions from the Fe 3d, Cr 3d and Cu 3d states to the VBs of both compounds. These measurements provide information primarily on the transition metal 3d partial density of states (DOS) in the valence band. In addition, S $L_{2,3}$ (3s3d $\rightarrow$ 2p transition) and S K$\beta_{1,3}$ (3p $\rightarrow$ 1s transition) spectra were measured in order to probe the S 3s3d and S 3p occupied DOS, respectively. The energy scales of all XES spectra relative to the Fermi level were calibrated using the binding energies of relevant initial (core-level) states determined by XPS. Figures 5(a) and (b) show the XES spectra compared with the XPS VB spectra. The XPS VB and XES spectra are clearly consistent: the feature of the XPS VBs at ∼1–1.5 eV is close to the intensity maximum of the Cr Lα XES, while the features at 2, 4, 6 and 13 eV are close to the maxima of the Cu Lα, S K$\beta_{1,3}$, Fe Lα and S $L_{2,3}$ XES, respectively.

3.3. Band structure calculations

In a recent calculation by Min Sik Park *et al* [7], the electronic structure of both compounds has been calculated in the local density approximation (LDA) as well as in the LDA + U approach.

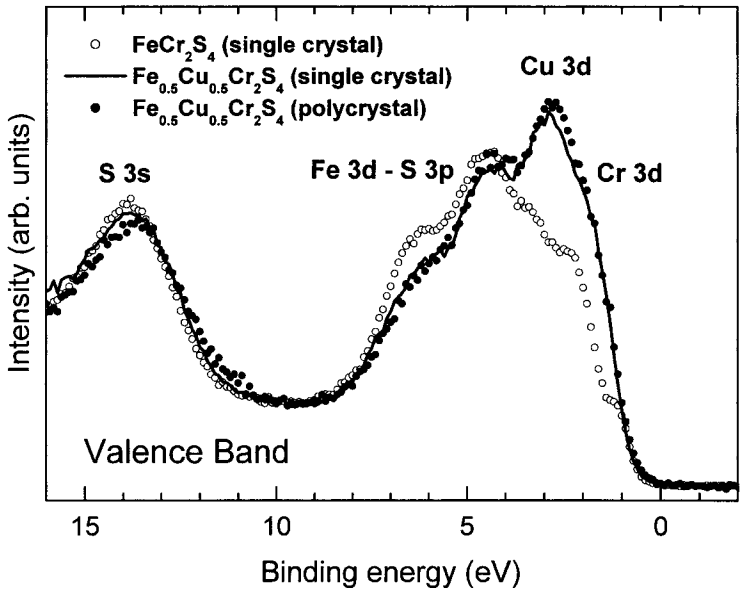

Figure 4. XPS VB spectra of $FeCr_2S_4$ and $Fe_{0.5}Cu_{0.5}Cr_2S_4$.

Only the LDA + U results for the density of states were reported [7], but, due to quite moderate values of on-site Coulomb interaction parameters used, one can note a reasonable agreement with our results, obtained in the LDA with gradient corrections. The main effect of an inclusion of on-site Coulomb correlation in the LDA + U method is the lowering of the energy of affected occupied bands and raising the energy of empty bands, which may result in a gap opening at the Fermi level. However, the thiospinel materials under consideration do not provide a clean choice of localized states where such treatment of correlation effects would be physically well justified. The search for correlation parameters at Fe, Cr and Cu sites simultaneously is hardly possible within a self-contained scheme, so that the LDA + U treatment in this case remains rather an *ad hoc* tool for obtaining a semiconducting behaviour, that was not a concern of our study. In agreement with the LDA result mentioned in [7], we found $FeCr_2S_4$ to be half-metallic, with a (tiny) band gap in the majority-spin states. $Fe_{0.5}Cu_{0.5}Cr_2S_4$, contrary to the result of [7], was not found to be an insulator according to the LDA calculation—most probably due to different structures used in both calculations. Min Sik Park *et al* [7] apparently used the cubic spinel structure in their calculation, and the study of the $Fe_{0.5}Cu_{0.5}Cr_2S_4$ material presumed some periodic distribution of Fe and Cu atoms over tetrahedral sites, not explicitly specified in the publication. In the present calculation, we used the crystal structure data as specified above, that differs from the standard spinel structure. Most importantly, the ordering of Fe and Cu sites has been properly taken into account. As a result, we found $Fe_{0.5}Cu_{0.5}Cr_2S_4$ to be a half-metal, similarly to $FeCr_2S_4$. But in contrast to the latter system, a pseudogap is seen in the minority-spin channel, which increases the chances of this material becoming semiconducting (due to additional structure distortion, or correlation effects).

Our calculated total densities of states for both systems are shown in figure 6. The shaded part represents occupied states, that can be compared with the XPS data. The broadening of calculated DOS with the half-width parameter 0.25 eV (that roughly corresponds to the spectrometer resolution and with photoionization cross-sections of individual atoms [23] taken into account) is shown as a thick line. The agreement between the position of major features in

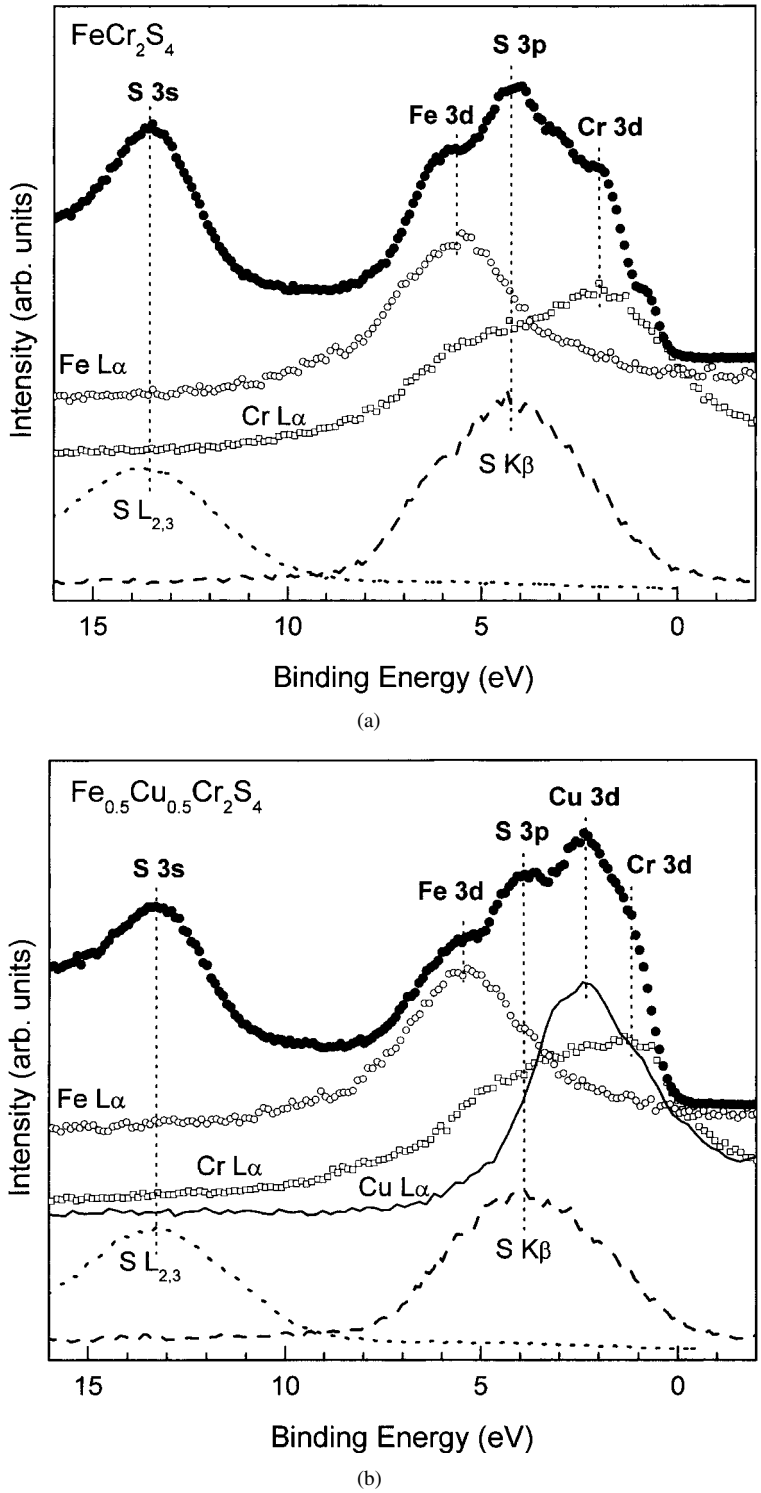

Figure 5. Comparison of XPS VB with XES spectra of constituents for the single crystals: $FeCr_2S_4$ (a) and $Fe_{0.5}Cu_{0.5}Cr_2S_4$ (b).

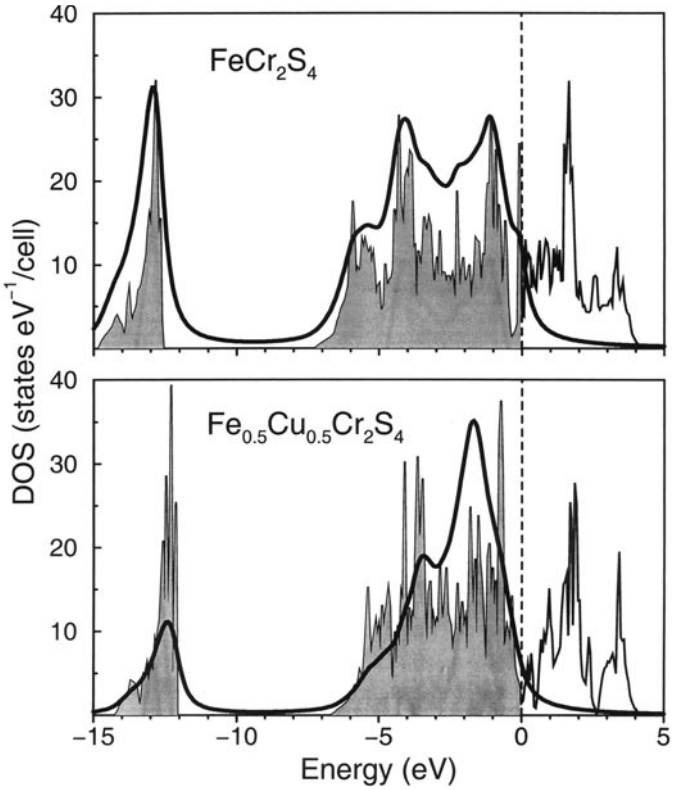

Figure 6. Calculated total densities of states for $FeCr_2S_4$ and $Fe_{0.5}Cu_{0.5}Cr_2S_4$. The occupied DOS broadened with the half-width of 0.25 eV is shown by a thick line.

the measured XPS spectra (figures 5(a) and (b)) and calculated DOS (figure 6), with partial spin-resolved DOS as shown in figure 7 taken into account, allows identification of the composition of the valence band without ambiguity. An important difference between the XPS data for the two materials is the presence of a step (resembling a Fermi edge) near the bottom of the valence band in $FeCr_2S_4$, which is completely missing in $Fe_{0.5}Cu_{0.5}Cr_2S_4$. From the analysis of the partial DOS shown in figure 7, the origin of this feature can be clearly traced to the minority-spin state of Fe. The energy position of the peak in the photoemission spectrum associated with S 3s states is reproduced in the calculation with much better accuracy than is typical for a similar feature in oxides, due to lower localization of the S 3s state as compared to the O 2s.

In $Fe_{0.5}Cu_{0.5}Cr_2S_4$, the sulphur atoms in two crystallographically inequivalent positions (S1 being bonded to Fe and Cr whereas S2 to Cu and Cr) exhibit slightly different DOS distribution related to their 3s states. However, in the energy region shown in figure 7 the difference between their 3p DOS distribution is quite small, so that merely an average DOS at the S site is shown. For both systems, the feature in the valence-band photoemission spectrum at the binding energy of $\sim$6 eV can be clearly associated with majority-spin Fe 3d states (where a large exchange splitting, associated with a magnetic moment of $\sim$3.00 μ_B, is present). The magnetic moments at Cr sites are antiparallel to the Fe moments and also anomalously large (2.75 μ_B), in agreement with measured neutron diffraction values as mentioned above.

Equally good agreement holds for the $Fe_{0.5}Cu_{0.5}Cr_2S_4$ system. There is no clear effect on the partial Fe 3d and Cr 3d states related to the presence of copper. The Cu 3d states

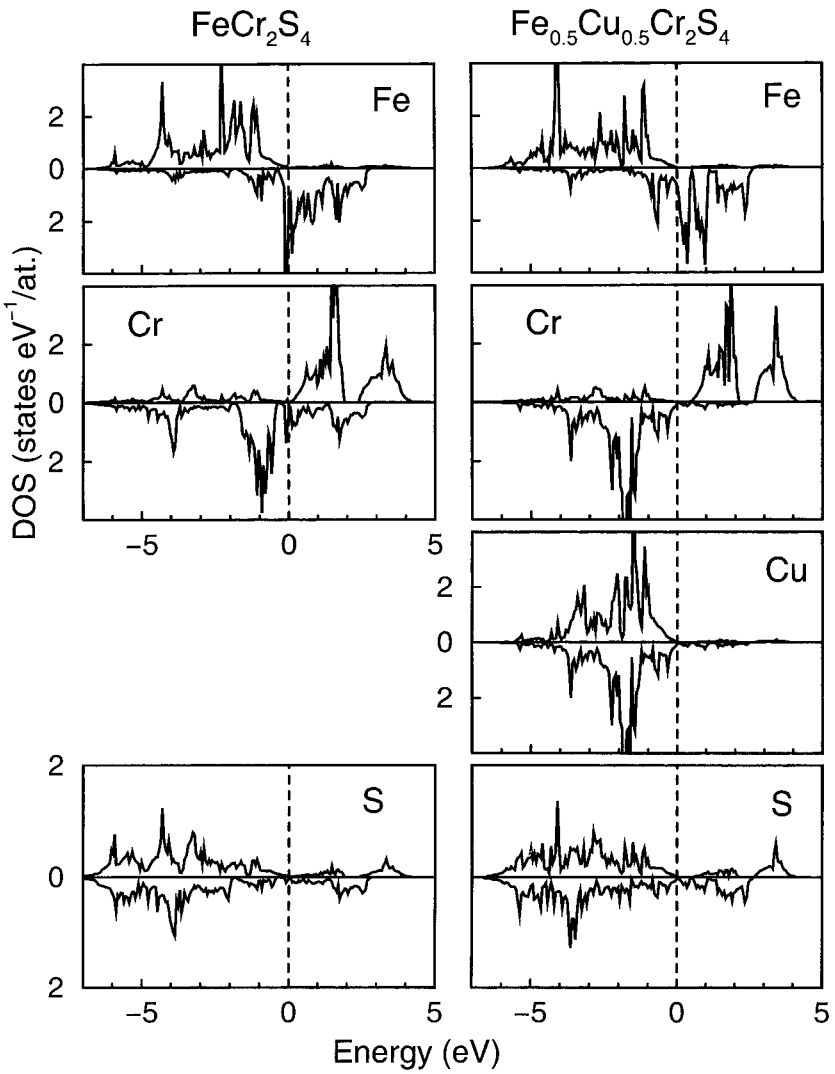

Figure 7. Calculated spin-resolved partial densities of states for $FeCr_2S_4$ and $Fe_{0.5}Cu_{0.5}Cr_2S_4$.

are not affected by magnetic splitting and remain relatively well localized, contributing to the photoelectron spectrum mostly near the binding energies 2–3 eV.

Due to the higher energy position of the Cr 3d states and smaller exchange splitting than for the Fe 3d, the Cr 3d states contribute to the photoelectron spectrum mainly in the binding energy region of 1–2 eV.

The identification of the features in the valence-band XPS, consistent with the band structure calculation results, is also supported by the x-ray emission data discussed above.

4. Conclusions

A full study of the electronic structure of $Fe_{1-x}Cu_xCr_2S_4$ ($x = 0$ and 0.5), including measurements of x-ray emission and photoelectron spectra and first principles band structure

calculations, has revealed that in $FeCr_2S_4$ the valence band comprises Fe 3d, Cr 3d and S 3p states. The VB states below the Fermi level are dominated by the Cr 3d contribution, but there are minority-spin Fe 3d states that produce a clear Fermi step in the photoelectron spectrum. Otherwise, Fe 3d and S 4p states are represented at slightly lower energies. The substitution of Cu for Fe results in the introduction of Cu^+ ions. The band structure calculations based on the correct ordered distribution of Fe and Cu on the tetrahedral sites yields different DOS for the two distinct S species. The valence band of $Fe_{0.5}Cu_{0.5}Cr_2S_4$ appears similar to that of $FeCr_2S_4$, but there is an additional contribution from the Cu 3d states just below the Cr 3d states. This study has therefore provided new information about the band description of these important materials, and has resolved many of the questions raised by earlier studies [3, 4, 7].

Acknowledgments

This work was supported by the Russian State Programme on Superconductivity, Russian Science Foundation for Fundamental Research (project 96-15-96598 and 98-02-04129), NATO Linkage Grant (HTECH.LG 971222) and DFG-RFFI project. We also thank EPSRC for financial support (HMP).

References

[1] Ramirez A P, Cava R J and Krajewski J 1997 *Nature* **386** 156
[2] Palmer H M and Greaves C 1999 *J. Mater. Chem.* **9** 637
[3] Haacke G and Beegle L C 1967 *J. Phys. Chem. Sol.* **28** 1699
[4] Lotgering F K, van Stapele R P, van der Stehen G H A M and van Wieringen J S 1969 *J. Phys. Chem. Sol.* **30** 799
[5] Lotgering F K and van Stapele R P 1967 *Solid State Commun.* **5** 143
[6] Goodenough J B 1969 *J. Phys. Chem. Sol.* **30** 261
[7] Park Min Sik, Kon S K, Youn S J and Min B I 1999 *Phys. Rev.* B **59** 10 018
[8] Kurmaev E Z, Fedorenko V V, Shamin S N, Postnikov A V, Wiech G and Kim Y 1992 *Phys. Scr.* T **41** 288
[9] Dolgih V E, Cherkashenko V M, Kurmaev E Z, Goganov D A, Ovchinnikov E K and Yarmoshenko Yu M 1984 *Nucl. Instrum. Methods* **224** 117
[10] Andersen O K and Jepsen O 1984 *Phys. Rev. Lett.* **53** 2571
[11] Andersen O K, Jepsen O and Sob M 1997 *Electronic Band Structure and its Applications (Springer Lecture Notes in Physics 283)* (Berlin: Springer)
[12] Andersen O K 1994 *Methods of Electronic Structure Calculations* (Singapore: World Scientific)
[13] Palmer H M and Greaves C in preparation
[14] von Barth U and Hedin L 1972 *J. Phys. C: Solid State Phys.* **5** 1629
[15] Langreth D C and Mehl M J 1981 *Phys. Rev. Lett.* **47** 446
[16] Langreth D C and Mehl M J 1983 *Phys. Rev.* B **28** 131
[17] Ok H N, Baek K S, Lee H S and Kim C S 1990 *Phys. Rev.* B **41** 62
[18] Steiner P, Kinsinger V, Sander I, Siegwart B, Hufner S, Politis C, Hoppe R and Muller H P 1987 *Z. Phys.* B **67** 497
[19] Hufner S, Steiner P, Weirich M and Courths R 1991 *Z. Phys.* B **85** 43
[20] Tsurkan V, Demeter M, Hartmann D and Neumann M *Solid State Commun.* **114** 149
[21] Lu Z E *et al* 1996 *Phys. Rev.* B **53** 9626
[22] Kurmaev E Z *et al* 1998 *J. Phys.: Condens. Matter* **10** 1687
[23] Yeh J J and Lindau I 1985 *At. Data Nucl. Data Tables* **32** 1